

From Data to Diagnosis: A Large, Comprehensive Bone Marrow Dataset and AI Methods for Childhood Leukemia Prediction

Running title

Bone Marrow Dataset & Methods for Childhood Leukemia

Authors

Henning Höfener^{1*}, Farina Kock¹, Martina Pontones², Tabita Ghete^{2,3}, David Pfrang¹, Nicholas Dickel⁴, Meik Kunz⁴, Daniela P Schacherer¹, David A Clunie⁵, Andrey Fedorov⁶, Max Westphal¹, Markus Metzler^{2,3,7}

¹ Fraunhofer Institute for Digital Medicine MEVIS, Bremen, Germany

² Department of Pediatrics and Adolescent Medicine, University Hospital Erlangen, Erlangen, Germany

³ Bavarian Cancer Research Center (BZKF), Erlangen, Germany

⁴ Medical Informatics, Friedrich-Alexander University of Erlangen-Nürnberg, Erlangen, Germany

⁵ PixelMed Publishing LLC, Bangor, PA, USA

⁶ Department of Radiology, Brigham and Women's Hospital and Harvard Medical School, Boston, MA, USA

⁷ Comprehensive Cancer Center Erlangen-EMN (CCC ER-EMN), Erlangen, Germany

* Corresponding author (henning.hoefener@mevis.fraunhofer.de)

From Data to Diagnosis: A Large, Comprehensive Bone Marrow Dataset and AI Methods for Childhood Leukemia Prediction

Abstract

Leukemia diagnosis primarily relies on manual microscopic analysis of bone marrow morphology supported by additional laboratory parameters, making it complex and time consuming. While artificial intelligence (AI) solutions have been proposed, most utilize private datasets and only cover parts of the diagnostic pipeline. Therefore, we present a large, high-quality, publicly available leukemia bone marrow dataset spanning the entire diagnostic process, from cell detection to diagnosis. Using this dataset, we further propose methods for cell detection, cell classification, and diagnosis prediction. The dataset comprises 246 pediatric patients with diagnostic, clinical and laboratory information, over 40 000 cells with bounding box annotations and more than 28 000 of these with high-quality class labels, making it the most comprehensive dataset publicly available. Evaluation of the AI models yielded an average precision of 0.96 for the cell detection, an area under the curve of 0.98, and an F1-score of 0.61 for the 33-class cell classification, and a mean F1-score of 0.90 for the diagnosis prediction using predicted cell counts. While the proposed

approaches demonstrate their usefulness for AI-assisted diagnostics, the dataset will foster further research and development in the field, ultimately contributing to more precise diagnoses and improved patient outcomes.

Introduction

Bone marrow (BM) morphology is the basis for the assessment of hematopoiesis and many systemic diseases. In cancer research, BM morphology can be used to analyze both physiological changes in organ function and pathological processes in neoplasia. These changes are reflected in quantitative and qualitative effects that can only partially be captured by the current analog approach. In clinical practice, BM collection, preparation, and analysis is still largely manual and dependent on the available equipment, the used procedures, and the experience of the medical staff. This variability limits the comparability of manually collected data and can lead to uncertainties in disease classification(1). The diagnosis of leukemia for both children and adults can typically be made based on the manual differential cell count (DCC) of approximately 100-200 nucleated BM cells in a bone marrow aspirate (BMA) smear. DCC is routinely performed by specially trained hematologists with years of experience, but the process can be slow, error-prone, and resource-intensive. Furthermore, the distinction of some therapeutically relevant subtypes requires not only BM morphology, but also additional clinical and laboratory parameters(2). Due to the complexity of the data, the diagnostic process for leukemia is challenging and is highly dependent on the experience of the clinicians involved.

Therefore, automation of these processing steps by artificial intelligence (AI) models has the potential to overcome the current limitations of BM analysis. Several approaches of AI-based detection and classification of BM cells, as well as diagnosis predictions have already been proposed. We have previously published a comprehensive review of current AI

approaches(3). The training of high-performing AI models and their evaluation require large and high-quality datasets. However, most datasets used in the literature are kept private. Only few adequately sized datasets have been published so far. For BM cell detection, Eckardt, Schmittmann, et al.(4) released a dataset containing ~5k cells in 62 regions of interest (ROI) images. For cell detection in peripheral blood, a number of smaller datasets ranging from ~1.5k to ~40k cells have been published(5–7). While more datasets exist for cell classification, only few incorporate more than 10k cells and more than 10 cell classes(4,8–10). Of these, Matek et al.'s dataset(9) gained the most traction and has been used for developing several classification approaches(11–17). Datasets aimed at leukemia diagnosis prediction that feature blood or BM image data are particularly scarce and focus only on adult leukemia patients(14,18,19).

While the fundamental principles of BM analysis remain consistent across both children and adults, the absence of datasets specifically targeting childhood leukemia is a significant limitation, given the reported variations in the distribution of specific leukemia types in childhood(20–22). Furthermore, all of the mentioned datasets are only suitable for parts of the processing steps listed above.

This work presents a large and comprehensive dataset for the analysis of BMA smears from 246 pediatric patients with leukemia. It encompasses over 40 000 cell annotations and high-quality, fine-grained class labels for more than 28 000 cells, obtained through a consensus approach from five hematology experts. It is the first dataset of this size to integrate three pivotal steps of the leukemia diagnosis process: cell detection, cell classification, and diagnosis prediction. In addition, this work introduces a suite of capable methods for these three processing steps, which have been trained and evaluated using this dataset.

Methods

Dataset

This study retrospectively selected a cohort of 246 patients who met the inclusion criteria. The criteria required patients to be diagnosed with acute myeloid leukemia (AML), chronic myeloid leukemia (CML), or acute lymphoblastic leukemia (ALL) and to be under 18 years old at the time of initial diagnosis. Additionally, we required a BMA smear stained using the Pappenheim staining method to be available at the initial diagnosis, prior to any treatment. Please refer to Supplement 1 for a comprehensive list of inclusion criteria, along with a detailed list of task-specific exclusion criteria. This research has been approved by the ethics committee of the Friedrich-Alexander-University Erlangen-Nuernberg (Application 22-148-Br). All participants have given written informed consent.

BMA smears were digitized using a 3DHistech Panoramic MIDI II whole slide scanner with 40x objective lens (without immersion), resulting in a resolution of 0.11x0.11 $\mu\text{m}/\text{pixel}$. Two smears were digitized with a 3DHistech Panoramic 250 Flash scanner. All images were initially saved as proprietary MRXS format files, but afterwards converted to standard DICOM format for sharing.

Square regions of interest (ROI) of 2048 pixels edge length with well-spread (individually separated) cells were annotated on most of the digitized BMA smear 40x images. To generate the cell detection dataset, for a subset of the ROIs, all leukocytes within it were delineated with bounding box annotations. For the classification dataset, single-cell images of 256x256 pixels were extracted from the center of each bounding box. In cases where a cell exceeded these dimensions, a square image was extracted containing the complete bounding box. Images larger than 4096 pixels were downsampled afterwards. To enhance

the dataset, we further included some erythrocytes, thrombocytes, and rare cell types from various areas of the smears following the same procedure as outlined above.

To achieve high quality yet efficient cell class labeling of the single-cell images, we used a custom consensus approach, where each image is successively annotated by different observers until two requirements are met: An image must be annotated by at least two observers and the majority class must be selected in at least half of all annotations for that image. This consensus labelling approach was implemented as a multi-user web application that was developed for this purpose. The labeling view was particularly designed for high efficiency. Assigning a class label only requires a single click in the hierarchical, color-coded class tree. Figure 1 shows a screenshot of the labeling view of the annotation application. For the second observation of the cells, a validation mode was implemented. In this mode, cells that have been assigned to a particular cell class are displayed in a gallery view. This allows observers to check the gallery for cells that they consider to be incorrectly labeled and correct them. Although this procedure might introduce confirmation bias, it was incorporated to enhance the efficiency of the annotation process.

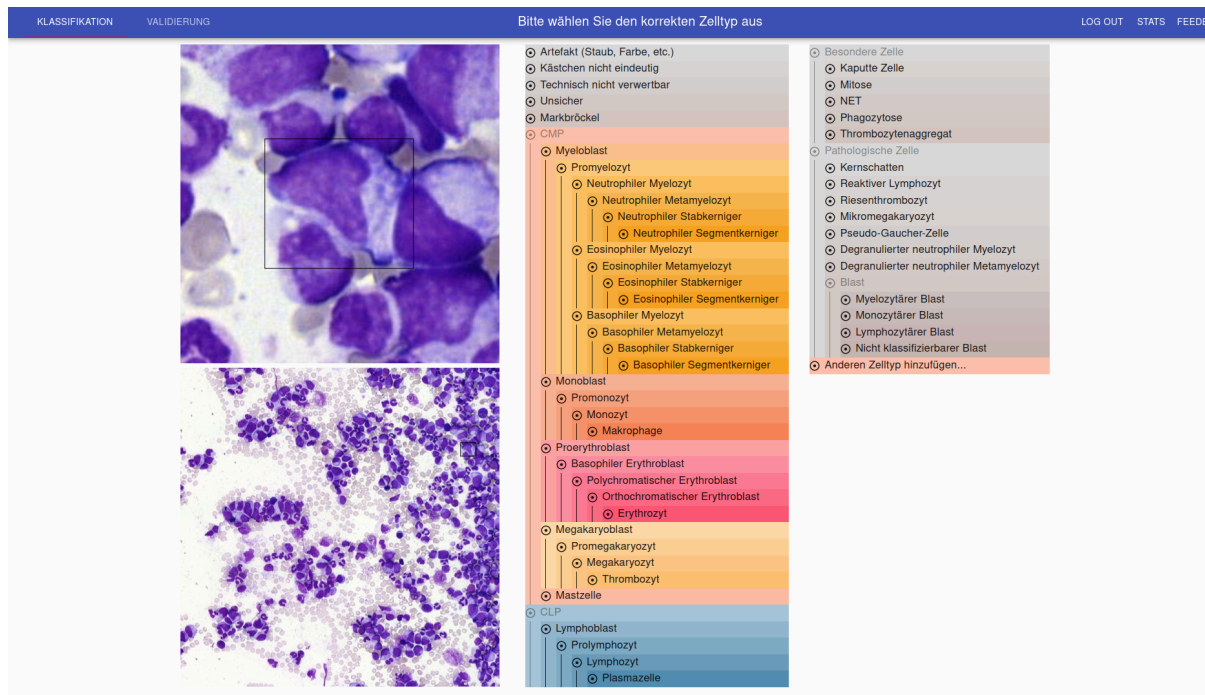


Figure 1: Web application for cell labeling. The screenshot shows the labeling view with the single-cell image and an overview image on the left, as well as a color-coded class tree on the right.

The annotation application was implemented to assign cells to one of >50 classes. For cell classification, we mapped it to 33 classes, as several classes had too few samples (Supplemental Table 1). The cells for which a consensus was reached comprise the cell classification dataset.

The ROIs, bounding boxes, and cell class annotations were stored in an internal proprietary format/database, and for sharing have been converted into a standard DICOM annotation format.

Clinical data was collected including leukemia type and subtype, gender and age (in intervals). Laboratory values also include the manual DCC as reported during clinical routine. Data was gathered from multiple different information systems, where not all requested parameters were necessarily available. Accordingly, the laboratory data contains

a considerable number of missing values. Thus, a trade-off between clinical relevance and the completeness of the features had to be determined. This resulted in a total of 18 laboratory values (Supplemental Table 2).

The dataset was partitioned into a training, a validation, and a test set at patient level using 60%, 20%, 20% of patients, respectively. This process was executed in a two-step manner. Initially, each patient was allocated to one of the sets with the objective to achieve an equitable distribution of diagnoses across all sets. Subsequently, patients with the same diagnoses were swapped between sets, ensuring that the cell class distribution across all sets was as close as possible. This manual process was implemented to ensure that the sets exhibited similar distributions of both diagnoses and cell classes, thereby ensuring that they are suitable for all tasks of the analysis pipeline. The specific stratification of patients into the sets is documented in Supplemental Table 3.

Automated Differential Cell Count

While some approaches integrate cell detection and classification into a single model, we opted to train two separate models for these tasks. This allows for individual and decoupled optimization and evaluation of each stage and improves comparability to other methods.

For the cell detection, we used two different state-of-the-art approaches being CenterNet(23) and Faster R-CNN (FRCNN)(24). The CenterNet uses an ImageNet-pretrained ResNet-50 backbone and outputs objects of a single class. It was trained for 50 epochs with Adam optimizer ($\text{lr}=1\text{e-}4$). The images were augmented using standard methods. The confidence threshold was optimized using the validation set. For prediction, local maxima within a distance of 10 pixels were considered. The FRCNN approach uses a COCO-pretrained ResNet-50 backbone and was used to output bounding box predictions only. It was trained for 250 epochs using stochastic gradient descent as the optimizer ($\text{lr}=1\text{e-}3$). The number of box detections per image was set to 544, representing the maximum number of bounding

boxes per image based on the training and validation sets. The non-maximum suppression threshold for the prediction head was reduced to 0.3 to suppress the output of bounding boxes with a larger overlap. Since the ROIs only contain well-spread cells, there is minimal or no overlap of cells in the dataset. We applied random flip, rotation, resizing, color jittering, and noise addition for data augmentation. We measured precision, recall, and F1-score as well as the average precision (AP) to compare and evaluate the cell detection models.

To classify the cells into 33 classes, we trained an ImageNet-pretrained ResNet-50 where we replaced the final linear layer with a dropout layer (dropout rate 0.2) followed by a concatenation layer where the output of the dropout is fused with the normalized resolution value that was stored alongside the single-cell images. This was then fed into a multilayer perceptron with one hidden layer of size 32 and an output layer with 33 class outputs. The model was trained with cross entropy loss for 85 epochs using the AdamW optimizer ($\text{lr}=3\text{e-}4$) and a batch size of 32. Learning rate was reduced ($\times 10$) if no improvement in the validation median F1-score was observed for 10 epochs. No class balancing was applied and the best model was selected according to the median F1-score on the validation set. The images are augmented as described above. Larger images were then downsampled to 256x256 pixels, then a random crop of 244x244 pixels was extracted. The cell classification approaches were compared and evaluated using the median and mean of the per-class F1-scores. Additionally, we evaluate both top 1 and top 2 accuracy (micro average) as well as the area under the receiver operating characteristic curve (AUROC; macro-average, one-vs-rest).

Diagnostic Models

For determining the leukemia type of patients, we trained machine learning models to distinguish between AML, ALL and CML. As input features for our models, we used both manual DCCs created by hematology experts as part of clinical routine and automated

DCCs predicted by our cell detection and cell classification model pipeline. To compare the predictive performance of the manual and the automated DCC, we trained separate models for these two feature sets. Furthermore, we used a set of 18 laboratory values that are typically assessed in the context of leukemia diagnosis, to train a stand-alone model, using only lab values, and to train models using both lab values and DCCs. This allows us to evaluate the performance and importance of the different feature sets for leukemia diagnostics. The F1-score was chosen as the primary metric for comparison and evaluation of diagnostic models.

For diagnosis prediction we used gradient boosting as it is considered state-of-the-art for tabular data(25). We used grid search and a repeated holdout split (20 iterations) stratified by leukemia subtype to tune the hyperparameters of the HistGradientBoostingClassifier. While far more efficient methods exist for hyperparameter optimization (e.g. Bayesian optimization), grid search was deemed feasible due to the small size of our dataset.

Statistical Analysis

To quantify uncertainty in any performance estimates, we used the bias-corrected and accelerated (BCa) bootstrap approach with 1000 bootstrap iterations to calculate 95% confidence intervals. This nonparametric method is applicable to all metrics for the different tasks. Some of the main advantages of BCa bootstrap confidence intervals compared to competing approaches are that they are transformation-respecting and second order accurate in terms of their coverage probability(26). We employed a hierarchical version of the BCa bootstrap to take into account the hierarchical structure of our data with multiple cells per patient similar to the approach of Saravan et al.(27). Due to the exploratory nature of our analyses, we did not apply an adjustment for multiplicity.

Results

Dataset

Our cohort consists of 246 patients with AML, ALL, or CML diagnosis (Figure 2a). The distribution of patients (54.2% male and 45.8% female of all patients with known sex) was very similar to the national incidence of pediatric leukemia with a ratio of male to female of 54.4% and 45.6%, respectively(28). The dataset comprises diagnostic information (leukemia type and subtype), manual DCCs and 18 laboratory parameters (Supplemental Table 3) from clinical routine, as well as digitized BMA smears for all of the 246 patients. We only considered data that was available at the time of diagnosis but before any treatment has been performed.

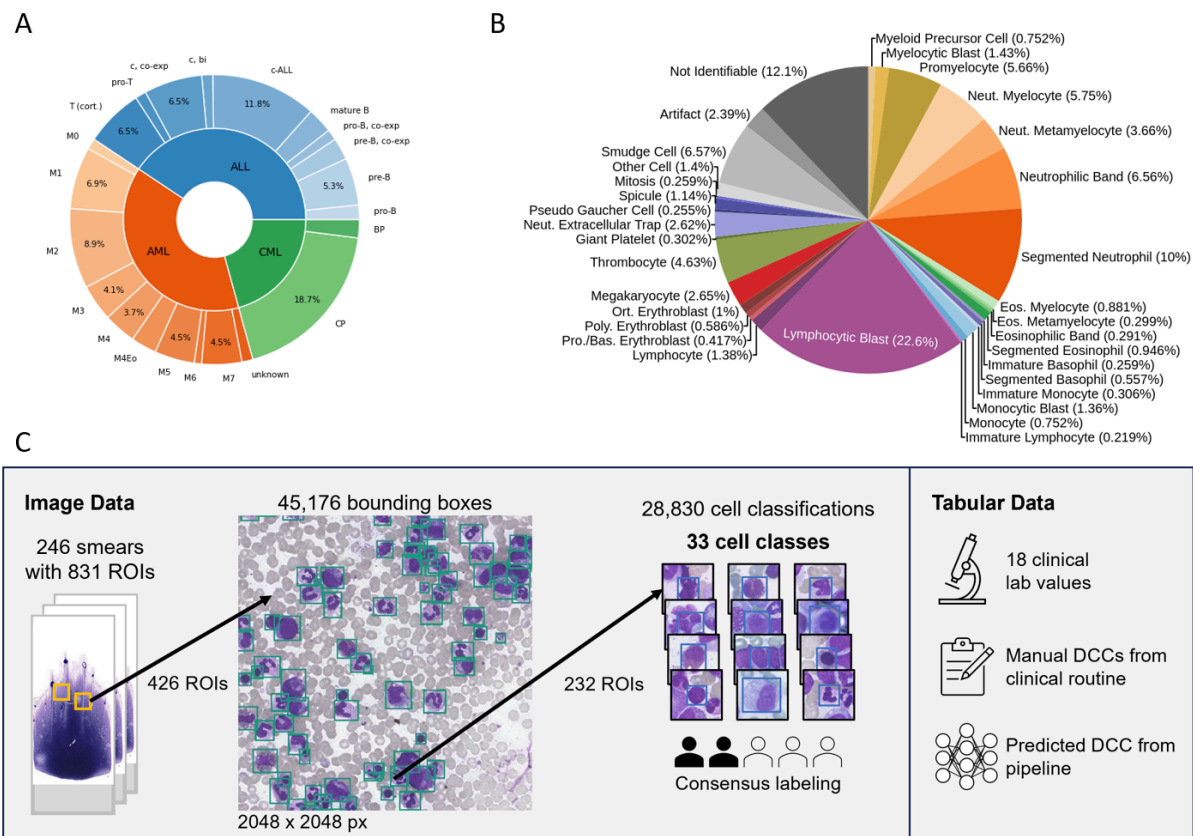


Figure 2: Overview of the structure and size of the dataset. A: Distribution of leukemia types and subtypes. B: Distribution of cell classes. C: Structure and size of the data and annotations.

A total of 831 ROIs were marked in the BMA smears. For 426 of them, all cells within the regions were exhaustively delineated using bounding boxes. For a subset of 232 of these ROIs, cell classes were annotated via a consensus labeling approach. This led to a total of 45,176 cells with bounding box annotations of which 28,830 cells also have class labels. Figure 2 visualizes the structure and size of the dataset.

To investigate the effect of our consensus labeling approach, we analyzed the annotations of the white blood cells performed by the five observers. For the majority of cells (87.8%) a consensus was already reached after two observations, which means that the first observation was confirmed by the second one. For another 8.4% of the cells consensus was reached after three observations. Here, the first two observations differed and the third

observation confirmed one of the two previous observations. Performing more observations only led to a consensus in an additional 0.4% of the cells. The remaining 3.3% could not reach a consensus label. Of these, the cells belonging to the test set were labeled through a consensus meeting. To quantify the effect of our labeling approach in contrast to having only a single observer, we analyzed how many consensus labels differ from the first annotation, very likely constituting a correction of that annotation. This is the case for 47.2% of those cells for which the first two observations differed, being 5.6% of all cells.

As our labeling workflow was designed for high efficiency, we measured the time between a cell being shown and the selection of a label in the list. As the web application was often left open during breaks, leading to very long labeling times, we use median values to give a realistic estimate of the actual labeling time. We report a median of 3 seconds in the classification view and 1.2 seconds in the validation view, per cell.

Automated Differential Cell Count

For cell detection, we evaluated both the CenterNet and the FRCNN. The results of the evaluation are listed in Table 1. The FRCNN clearly outperformed the CenterNet in all evaluated metrics.

Model	Precision	Recall	F1-score	Average Precision
CenterNet	0.890	0.904	0.897	0.919
FRCNN	0.967	0.945	0.956	0.958

Table 1: Precision, recall, F1-score, and average precision of the two cell detection approaches CenterNet and FRCNN for an intersection over union threshold of 0.5.

As shown in Table 2 and Figures 3 and 4, the cell classification shows a high prediction performance as visible in the confusion matrix. However, performance varies quite substantially between the classes, as can be observed in per-class F1-scores ranging from

0.000 (immature lymphocyte) to 0.945 (megakaryocyte). Performance is highly associated with the number of samples per class. 43% of classes with F1-scores below the median have less than 100 training samples, whereas this is only the case for 13% of the classes above the median. The high values of the top 2 accuracy indicate that the model is capable of learning the task but sometimes does not succeed in correctly ranking the top classes. The main reason is likely confusion between similar classes. This can also be observed in the confusion matrix, where we ordered the classes such that similar classes are close. Therefore, instead of a distinct diagonal, e.g. for eosinophils, the matrix builds up merely a block-like structure.

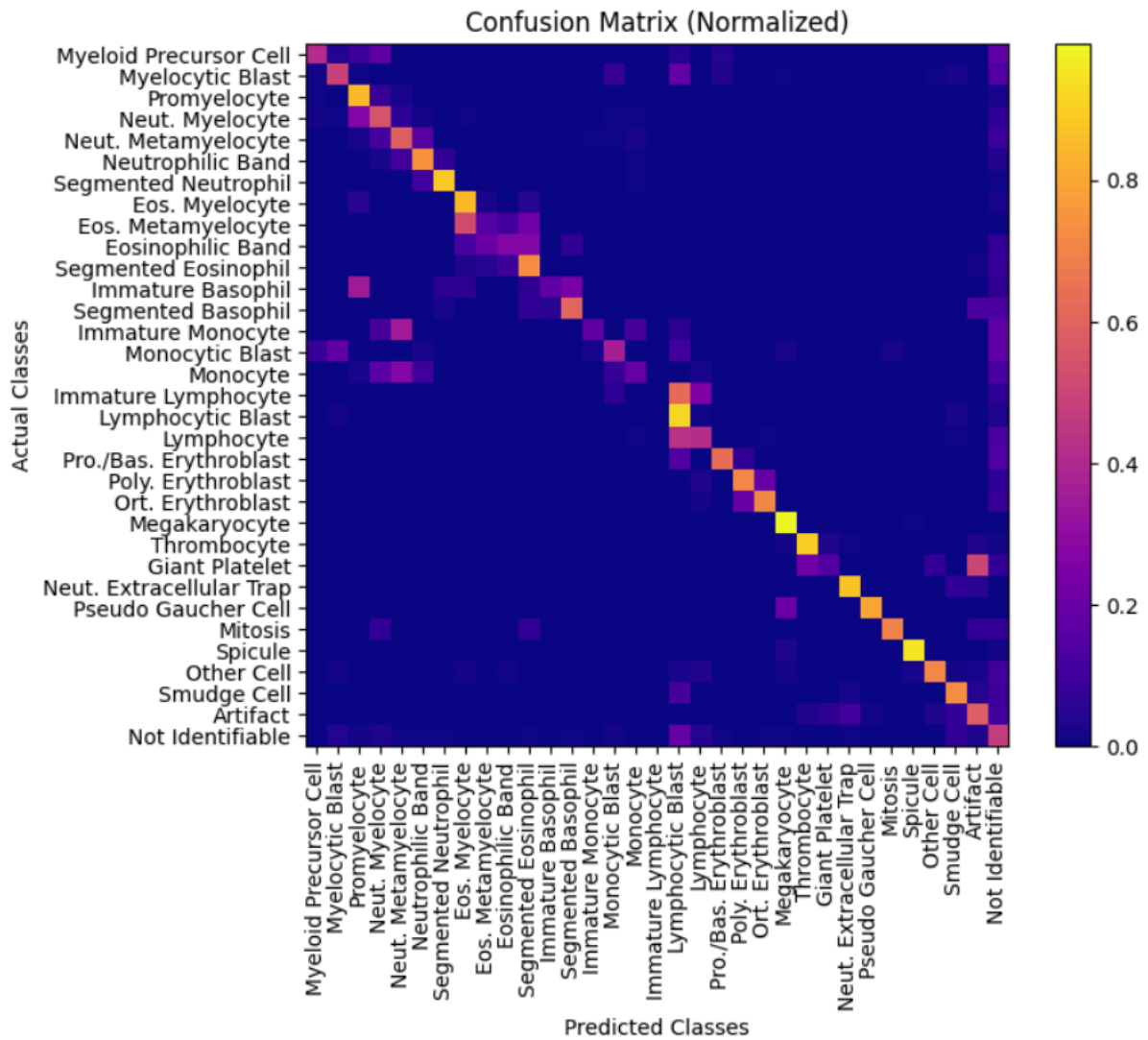


Figure 3: Confusion Matrix of the cell classification. Classes are ordered such that similar classes are close.

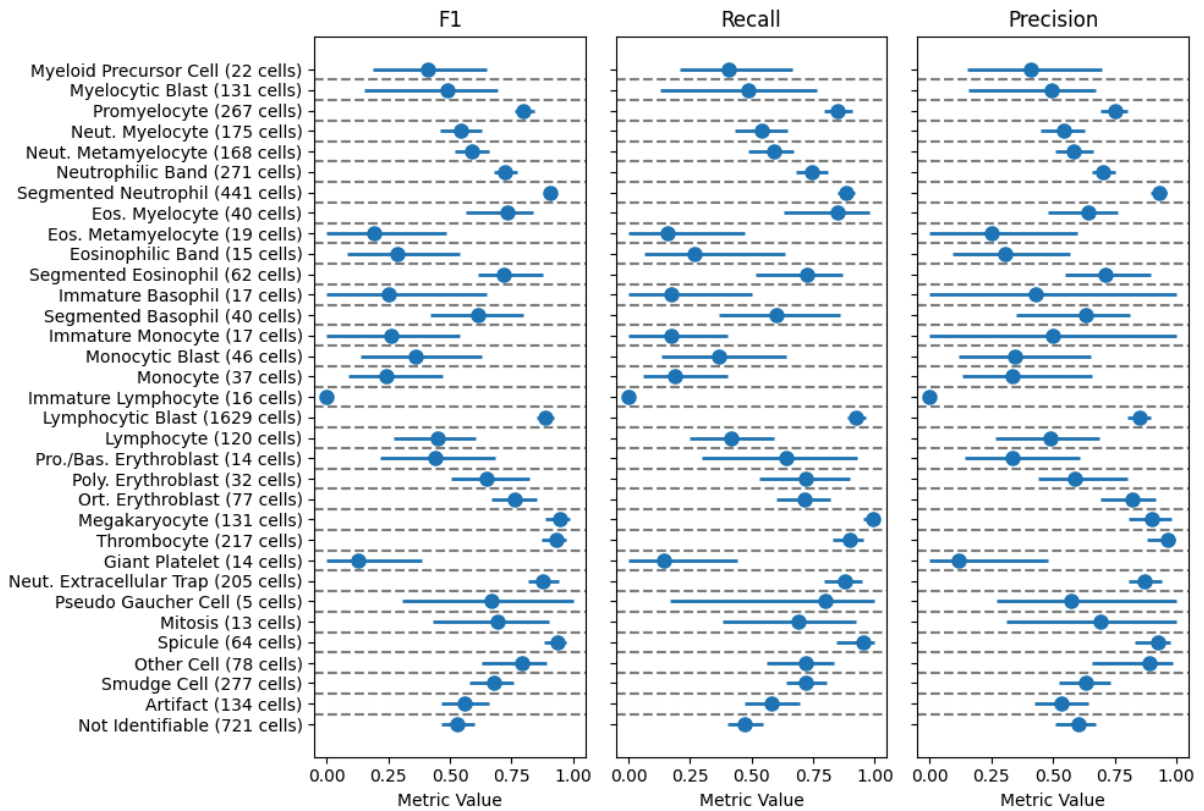


Figure 4: Visualization of the F1-scores, recall and precision values per cell class for the proposed cell classifier including 95% confidence intervals (BCa bootstrap, 1000 bootstrap iterations). The corresponding quantitative values are listed in supplemental Table 4.

As an external validation, we evaluated our approach using the dataset of Matek et al.(9). As this dataset only has one annotation per cell and the cell sizes are unknown, we modified our training procedure to not use this information (base model). To evaluate the effect of the proposed model vs. the base model, we also trained and evaluated the base model on our own dataset. Table 2 shows that our base model outperforms Matek. Furthermore, adding soft labels and cell masking appears to slightly improve the performance (Δ median F1 = 0.065; 95% CI: (-0.033, 0.124)). However, more test data would be required especially on rare cell classes to meaningfully measure this effect.

Model	Dataset	Median F1-score	Mean F1-score	Top 1 Accuracy	Top 2 Accuracy	AUROC
Matek	Matek et al.(9)	0.590	0.545	N/A	N/A	N/A
Base	Matek et al.(9)	0.749 (0.731 - 0.767)	0.671 (0.648 - 0.690)	0.873 (0.869 - 0.876)	0.961 (0.959 - 0.963)	0.990 (0.987 - 0.991)
Base	Ours	0.550 (0.497-0.606)	0.561 (0.534 - 0.591)	0.729 (0.700 - 0.767)	0.879 (0.858 - 0.899)	0.982 (0.978 - 0.985)
Proposed	Ours	0.615 (0.557 - 0.680)	0.577 (0.543 - 0.618)	0.748 (0.721 - 0.782)	0.890 (0.872 - 0.908)	0.981 (0.976 - 0.985)

Table 2: Aggregated performance metrics including 95% confidence intervals (BCa bootstrap, 1000 bootstrap iterations) for cell classification models. The upper part of the table shows the model as proposed by Matek et al.(9) (no confidence intervals available) compared to our base model (the proposed model without soft labels and cell masks) trained and evaluated using Matek et al.'s dataset. The lower part of the table shows our base model compared to the proposed model trained and evaluated using our dataset.

Diagnostic Models

We trained and evaluated three diagnostic models for leukemia prediction (target classes: ALL, AML, CML) trained with different sets of input features: laboratory values, DCCs from clinical routine, and predicted DCCs generated by our cell detection and classification models. To ensure a fair comparison, we only included patients for which all three kinds of input data are available, leading to 129 patients (64 ALL, 18 AML, 47 CML) in total. All models were evaluated on the test set (consisting of 32 patients) in terms of confusion matrices (Figure 5), as well as averaged performance measures (Table 3).

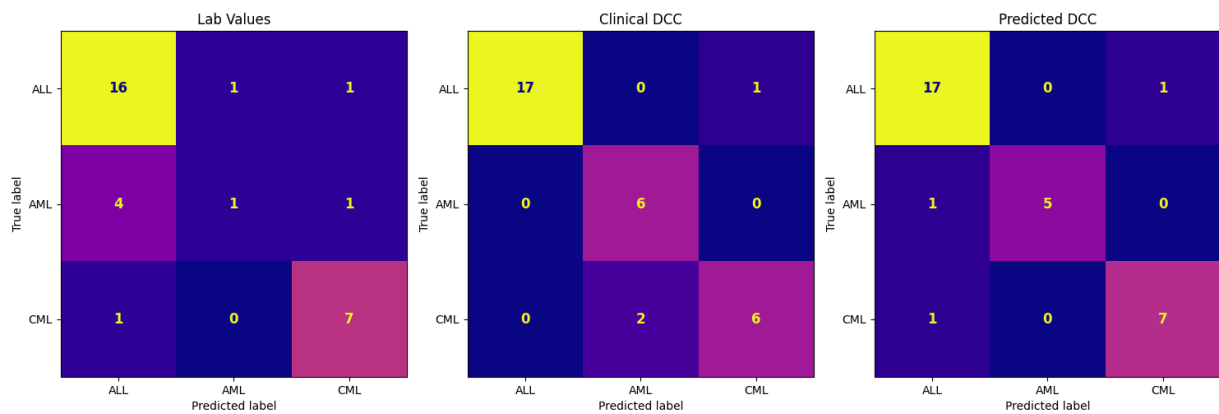


Figure 5: Confusion matrices on the test set for 3 diagnostic models using distinct sets of input features: laboratory parameters, DCCs from clinical routine, and predicted DCCs generated by our cell detection and classification models.

Model / Metric	F1-score ALL	F1-score AML	F1-score CML	Mean F1-score
Lab Values	0.821 (0.686 - 0.900)	0.250 (0.000 - 0.667)	0.824 (0.571 - 0.941)	0.631 (0.496 - 0.834)
Clinical DCC	0.971 (0.839-1.000)	0.857 (0.667 - 1.000)	0.800 (0.462 - 0.941)	0.876 (0.703 - 0.971)
Predicted DCC	0.919 (0.789 - 0.973)	0.901 (0.404 - 1.000)	0.875 (0.592 - 1.000)	0.901 (0.745 - 0.971)

Table 3: Mean and per-class F1 scores, including 95% confidence intervals (BCa bootstrap, 1000 bootstrap iterations) for uncertainty quantification.

While the lab values model has issues distinguishing ALL and AML patients, diagnostic models based on DCCs (both clinical and predicted) show better performance for ALL and AML (Table 3). The overall performance is similar for the predicted and clinical DCC models. Note that the high uncertainty in performance metrics is due to the small size of the test set.

We investigated whether using laboratory parameters and DCC data together yields better performance than using only DCCs. This was not the case on our dataset: exactly the same patients were misclassified after lab values have been added as further features, both for the clinical and the predicted DCCs.

Discussion

AI-based hemato-morphology is an emerging field. A large number of approaches have been proposed in recent years. However, most approaches acquire and use internal datasets that are not shared. This substantially limits both reproducibility and the overall progress in the field, as researchers cannot build upon existing datasets. Although there are some publicly available datasets, none has emerged as a standard. Matek et al.'s dataset(9) is closest to being a standard benchmark, but their dataset has some limitations such as partitioning into training and test sets in a non patient-stratified manner, which allows overlap between slides of both sets and may compromise generalizability of trained models(29).

We created a large, high-quality, publicly shareable dataset for hematology that provides images and labels for detection and classification of digitized BMA smears, as well as patient-level clinical information and laboratory data for leukemia type prediction. While there are publicly available datasets for each of those tasks, ours is the only one of that size to combine them all. Comparing our dataset to other publicly available datasets, we can state that with >40k white blood cells, it is the largest dataset for cell detection. The second largest

dataset comprises ~5k white blood cells(4). While there are larger datasets for cell classification with >92k cells(30) and >171k cells(9), our dataset is still large with >28k cells and is unique in that it employs a consensus labeling approach to ensure high-quality labels and is fine-grained to the extent that it distinguishes 33 different classes. In terms of diagnosis prediction, our dataset comprises 246 patients. A much larger cohort of 1251 AML patients with BMA smears was published for the prediction of NPM1 status(18). However, that dataset only contains a single leukemia type and only two laboratory values. In contrast, our dataset comprises three leukemia types with their subtypes and a set of 18 laboratory parameters.

But our dataset is not without limitations. Due to the considerable effort required to label a cell in a consensus meeting, only the cells from the test set were labeled in this manner. For the validation and training sets, these cells are designated as "no consensus found", which may impede the models' capacity to classify challenging samples. Also, as it is the case for virtually any dataset, a larger number of samples would have been beneficial. For both cell classes and leukemia subtypes, a substantial imbalance is observed, impeding the reasonable development of subtype classification models. While these limitations exist, our dataset nonetheless appears to be of exceptional value to the community.

Both steps of the automated DCC generation show high performance on the held-out test set, which was strictly kept unavailable for the development and optimization of the methods. The CenterNet and FRCNN approaches yield good detection results. The FRCNN's detection quality is comparable to that of the approach by Eckardt, Schmittmann et al.(4) with AP @ IoU<0.5 of 0.96 vs 0.97, confirming that the FRCNN approach is well suited for detecting leukocytes in BMA smears. While the FRCNN approach demonstrates superior performance metrics in comparison to CenterNet, the CenterNet remains a well-suited alternative in resource- and time-constrained environments.

The proposed cell classification approach shows high performance in the aggregated metrics. This is especially true given the very fine-grained classification task with 33 distinct classes. The approach also outperforms Matek et al.'s(9) classification model. However, difficulties for classes that share similar morphologies could be observed, as well as for classes with small sample sizes. The high top 2 accuracy shows that the model is capable of consistently ranking the correct class among its top predictions even if not always as the top choice.

Our diagnostic models are capable of distinguishing between ALL, AML, and CML, achieving a mean F1-score of 0.88 with clinical DCCs and 0.90 with predicted DCCs generated by our automated cell detection and classification pipeline. These results highlight the clinical potential of our DCC pipeline. The proposed set of 18 laboratory values alone does not effectively differentiate ALL from AML, nor does it provide additional value when combined with DCC data. This underscores the significance of DCC data as the most valuable feature for leukemia diagnostics, especially in the absence of genetic analysis, which is typically unavailable at the initial diagnosis stage.

The limited size of our dataset rendered the prediction of leukemia subtypes unfeasible. We distinguish 21 subtypes in our dataset (10 for ALL, 9 for AML, and 2 for CML), yet our reduced cohort of 129 patients used for training and evaluating diagnostic models lacked representation for some subtypes. Nonetheless, accurate diagnosis at the subtype level is crucial in clinical practice, for example in the distinguishing of acute promyelocytic leukemia, as treatment recommendations are contingent upon the specific subtype(31).

In this paper, we have introduced a large, high-quality pediatric leukemia bone marrow dataset along with methods for cell detection, classification, and diagnosis prediction. The dataset enables the development and evaluation of methods for the entire processing pipeline from cell detection through diagnosis prediction. To the best of our knowledge, it is the most comprehensive dataset for leukemia bone marrow analysis currently available.

Both proposed cell detection methods exhibit sufficient capability for real-world applications. The proposed cell classification approach yields high performance and outperforms Matek et al.'s(9) approach. Diagnostic models trained on the output of our cell classification pipeline are capable of distinguishing between ALL, AML and CML patients. This is a promising step in the direction of fully automated decision support in leukemia diagnostics.

Further extension of the dataset, particularly in regard to rare cell classes, is likely to enhance the automated DCC generation models. An expansion in leukemia types and subtypes would facilitate the development of diagnostic models for additional clinically relevant diagnostic classifications.

Data sharing statement

The dataset introduced in this work will be made publicly available through the National Cancer Institute Imaging Data Commons(32), with the dataset managed through Zenodo and available at <https://zenodo.org/records/15490664>, where an exemplar subset of the data is already published(33).

Acknowledgements

The authors thank Stefanie Barnickel, Nathalie Dollmann, Tatjana Flamann, Meinolf Suttorp, and Perdita Weller for the labelling of the cells.

The authors thank the following institutions for supplying BMA smears: University Hospital Augsburg (Univ.-Prof. Dr. Dr. med. Michael Frühwald), Charité Berlin - ALL-REZ BFM Study Group (PD Dr. med. Arend von Stackelberg), University Hospital at the Technical University Dresden (Prof. Dr. med. Meinolf Suttorp), University Hospital Essen - AML-BFM Study

Group (Prof. Dr. Dirk Reinhardt), Technical University of Munich (Prof. Dr. med. Irene Teichert-von Lüttichau), University Hospital Würzburg (Prof. Dr. med. Matthias Eyrich).

This study was supported by a grant from the German Federal Ministry of Education and Research (FKZ: 031L0262A; BMDDeep)

Preparation of the Dataset for publication was partly supported by Federal funds from the National Cancer Institute, National Institutes of Health (Task Order No. HHSN26110071 under Contract HHSN261201500003I).

Authorship Contributions

H.H., M.K., M.W., and M.M. designed the study; T.G. and M.P. acquired data and BMA smears and performed scanning; F.K., D.P., and N.D. curated patient data; H.H., F.K., and D.P. developed the AI methods; D.P. and M.W. performed statistical analysis; D.P.S., D.A.C., and A.F. performed integration of the dataset into IDC.

Disclosure of Conflicts of Interest

The authors declare no conflicts of interest.

References

1. Font P, Loscertales J, Soto C, Ricard P, Novas CM, Martín-Clavero E, et al. Interobserver variance in myelodysplastic syndromes with less than 5 % bone marrow blasts: unilineage vs. multilineage dysplasia and reproducibility of the threshold of 2 % blasts. *Ann Hematol.* 2015 Apr;94(4):565–73.

2. Arber DA, Orazi A, Hasserjian R, Thiele J, Borowitz MJ, Le Beau MM, et al. The 2016 revision to the World Health Organization classification of myeloid neoplasms and acute leukemia. *Blood*. 2016 May 19;127(20):2391–405.
3. Ghete T, Kock F, Pontones M, Pfrang D, Westphal M, Höfener H, et al. Models for the marrow: A comprehensive review of AI-based cell classification methods and malignancy detection in bone marrow aspirate smears. *HemaSphere*. 2024 Dec;8(12):e70048.
4. Eckardt JN, Schmittmann T, Riechert S, Kramer M, Sulaiman AS, Sockel K, et al. Deep learning identifies Acute Promyelocytic Leukemia in bone marrow smears. *BMC Cancer*. 2022 Feb 22;22(1):201.
5. Kouzehkhanan ZM, Saghari S, Tavakoli S, Rostami P, Abaszadeh M, Mirzadeh F, et al. A large dataset of white blood cells containing cell locations and types, along with segmented nuclei and cytoplasm. *Sci Rep*. 2022 Jan 21;12(1):1123.
6. Labati RD, Piuri V, Scotti F. All-IDB: The acute lymphoblastic leukemia image database for image processing. In: 2011 18th IEEE International Conference on Image Processing [Internet]. 2011 [cited 2024 Dec 4]. p. 2045–8. Available from: <https://ieeexplore.ieee.org/document/6115881>
7. Alipo-on JR, Escobar FI, Novia JL, Mana-ay S, Tan MJ, AlDahoul N, et al. Dataset for Machine Learning-Based Classification of White Blood Cells of the Juvenile Visayan Warty Pig [Internet]. IEEE; 2022 [cited 2025 Apr 17]. Available from: <https://ieee-dataport.org/documents/dataset-machine-learning-based-classification-white-blood-cells-juvenile-visayan-warty-pig>
8. Matek C, Schwarz S, Marr C, Spiekermann K. A Single-cell Morphological Dataset of Leukocytes from AML Patients and Non-malignant Controls [Internet]. The Cancer Imaging Archive; 2019 [cited 2025 Apr 17]. Available from: https://www.cancerimagingarchive.net/collection/aml-cytomorphology_lm/
9. Matek C, Krappe S, Münzenmayer C, Haferlach T, Marr C. Highly accurate differentiation of bone marrow cell morphologies using deep neural networks on a large image data set. *Blood*. 2021 Nov 18;138(20):1917–27.
10. Park S, Cho H, Woo BM, Lee SM, Bae D, Balint A, et al. A large multi-focus dataset for white blood cell classification. *Sci Data*. 2024 Oct 9;11(1):1106.
11. Alshahrani H, Sharma G, Anand V, Gupta S, Sulaiman A, Elmagzoub MA, et al. An Intelligent Attention-Based Transfer Learning Model for Accurate Differentiation of Bone Marrow Stains to Diagnose Hematological Disorder. *Life*. 2023 Oct;13(10):2091.
12. Aydin Atasoy N, Faris Abdulla Al Rahhawi A. Examining the classification performance of pre-trained capsule networks on imbalanced bone marrow cell dataset. *Int J Imaging Syst Technol*. 2024 May;34(3):e23067.
13. Glüge S, Balabanov S, Koelzer VH, Ott T. Evaluation of deep learning training strategies for the classification of bone marrow cell images. *Comput Methods Programs Biomed*. 2024 Jan;243:107924.
14. Hehr M, Sadafi A, Matek C, Lienemann P, Pohlkamp C, Haferlach T, et al. A morphological dataset of white blood cells from patients with four different genetic AML

- entities and non-malignant controls (AML-Cytomorphology_MLL_Helmholtz) [Internet]. The Cancer Imaging Archive; 2023 [cited 2025 Apr 17]. Available from: https://www.cancerimagingarchive.net/collection/aml-cytomorphology_mll_helmholtz/
15. Peng K, Peng Y, Liao H, Yang Z, Feng W. Automated bone marrow cell classification through dual attention gates dense neural networks. *J Cancer Res Clin Oncol*. 2023 Dec 1;149(19):16971–81.
 16. Tarquino J, Rodríguez J, Becerra D, Roa-Peña L, Romero E. Engineered feature embeddings meet deep learning: A novel strategy to improve bone marrow cell classification and model transparency. *J Pathol Inform*. 2024 Dec 1;15:100390.
 17. Tripathi S, Augustin AI, Sukumaran R, Dheer S, Kim E. HematoNet: Expert level classification of bone marrow cytology morphology in hematological malignancy with deep learning. *Artif Intell Life Sci*. 2022 Dec 1;2:100043.
 18. Eckardt JN, Middeke JM, Riechert S, Schmittmann T, Sulaiman AS, Kramer M, et al. Deep learning detects acute myeloid leukemia and predicts NPM1 mutation status from bone marrow smears. *Leukemia*. 2022 Jan;36(1):111–8.
 19. National Cancer Institute Clinical Proteomic Tumor Analysis Consortium (CPTAC). The Clinical Proteomic Tumor Analysis Consortium Acute Myeloid Leukemia Collection (CPTAC-AML) [Internet]. The Cancer Imaging Archive; 2019 [cited 2025 Apr 17]. Available from: <https://www.cancerimagingarchive.net/collection/cptac-aml/>
 20. Chaudhury SS, Morison JK, Gibson BES, Keeshan K. Insights into cell ontogeny, age, and acute myeloid leukemia. *Exp Hematol*. 2015 Sep;43(9):745–55.
 21. Janardan SK, Miller TP. Adolescents and young adults (AYAs) vs pediatric patients: survival, risks, and barriers to enrollment. *Hematology*. 2023 Dec 8;2023(1):581–6.
 22. Suttorp M, Millot F, Sembill S, Deutsch H, Metzler M. Definition, Epidemiology, Pathophysiology, and Essential Criteria for Diagnosis of Pediatric Chronic Myeloid Leukemia. *Cancers*. 2021 Feb 14;13(4):798.
 23. Zhou X, Wang D, Krähenbühl P. Objects as Points [Internet]. arXiv; 2019 [cited 2024 Feb 29]. Available from: <http://arxiv.org/abs/1904.07850>
 24. Ren S, He K, Girshick R, Sun J. Faster R-CNN: Towards Real-Time Object Detection with Region Proposal Networks. *IEEE Trans Pattern Anal Mach Intell*. 2017 Jun 1;39(6):1137–49.
 25. Borisov V, Leemann T, Seßler K, Haug J, Pawelczyk M, Kasneci G. Deep Neural Networks and Tabular Data: A Survey. *IEEE Trans Neural Netw Learn Syst*. 2024 Jun;35(6):7499–519.
 26. Carpenter J, Bithell J. Bootstrap confidence intervals: when, which, what? A practical guide for medical statisticians. *Stat Med*. 2000 May 15;19(9):1141–64.
 27. Saravanan V, Berman GJ, Sober SJ. Application of the hierarchical bootstrap to multi-level data in neuroscience. *Neurons Behav Data Anal Theory*. 2020;3(5):<https://nbdt.scholasticahq.com/article/13927-application-of-the-hierarchical-bootstrap-to-multi-level-data-in-neuroscience>.

28. Spix C, Erdmann F, Grabow D, Ronckers C. Childhood and adolescent cancer in Germany - an overview. *J Health Monit.* 2023 Jun;8(2):79–94.
29. Goldgof GM, Sun S, Van Cleave J, Wang L, Lucas F, Brown L, et al. DeepHeme: A generalizable, bone marrow classifier with hematopathologist-level performance. *BioRxiv Prepr Serv Biol.* 2023 Feb 21;2023.02.20.528987.
30. Chen Y, Zhu Z, Zhu S, Qiu L, Zou B, Jia F, et al. SCKansformer: Fine-Grained Classification of Bone Marrow Cells via Kansformer Backbone and Hierarchical Attention Mechanisms. *IEEE J Biomed Health Inform.* 2024;1–14.
31. Sanz MA, Fenaux P, Tallman MS, Estey EH, Löwenberg B, Naoe T, et al. Management of acute promyelocytic leukemia: updated recommendations from an expert panel of the European LeukemiaNet. *Blood.* 2019 Apr 11;133(15):1630–43.
32. Fedorov A, Longabaugh WJR, Pot D, Clunie DA, Pieper SD, Gibbs DL, et al. National Cancer Institute Imaging Data Commons: Toward Transparency, Reproducibility, and Scalability in Imaging Artificial Intelligence. *RadioGraphics.* 2023 Dec 1;43(12):e230180.
33. Höfener H, Kock F, Pontones MA, Ghete T, Pfrang D, Dickel N, et al. BoneMarrowWSI-PediatricLeukemia: A Comprehensive Dataset of Bone Marrow Aspirate Smear Whole Slide Images with Expert Annotations and Clinical Data in Pediatric Leukemia [Internet]. Zenodo; 2025 [cited 2025 Sep 15]. Available from: <https://zenodo.org/records/15490664>

Supplement

Supplement 1: Inclusion and Exclusion criteria

Global Inclusion Criteria for the Research Project

- Children and adolescents up to the age of 18 at the time of initial diagnosis
- Limited to acute and chronic leukemia, specifically AML, ALL, CML
- Availability of the bone marrow smear at the time of initial diagnosis
- Uniform staining of the bone marrow smear according to Pappenheim
- The bone marrow smear must not contain any anticoagulants
- Intact bone marrow smears with airtight coverslip
- Availability of all information on the slide (relevant only for patients from University Hospital Erlangen)
 - Smear date
 - Name of the patient
 - BM identification (to distinguish from peripheral blood smear)
- Sufficiently good image quality (judged by hematology experts)
- The time period of retrospective inclusion varies per leukemia type and data source:
 - Patients from University Hospital Erlangen:
 - CML: 2013-2022
 - AML: 2011-2020
 - ALL: 2013-2021
 - Patients from other clinics:
 - No specific time restriction. Cases for specific rare ALL- and AML-subtypes were requested. Collected cases range from 2005 to 2022.

Task-Specific Exclusion Criteria and Patient Numbers

- **Cell Detection**
 - Included: 211 / 246 patients
 - Excluded: 35 / 246 patients. Reasons:
 - No cell boxes annotated: 35 patients

- **Cell Classification**

- Included: 114 / 246 patients
- Excluded: 132 / 246 patients. Reasons:
 - No cell classes annotated: 132 patients

- **Diagnostic Models**

- Included: 129 / 246 patients
- Excluded: 117 / 246 patients. Exclusion criteria (some patients fulfill more than one criterion):
 - Found out later that patient has already been under treatment at time of initial smear: 1 patient
 - No lab values available (meaning none at all; as soon as at least 1 lab value is available, this exclusion criterion does not apply. For some patients, only 4 / 18 lab values are available.): 116 patients
 - No clinical DCC available: 67 patients

Supplemental Tables

Original Cell Type	Mapped Cell Type
Myeloid Precursor Cell	Myeloid Precursor Cell
Myelocytic Blast	Myelocytic Blast
Promyelocyte	Promyelocyte
Neutrophilic Myelocyte	Neutrophilic Myelocyte
Degranulated Neutrophilic Myelocyte	
Neutrophilic Metamyelocyte	Neutrophilic Metamyelocyte
Degranulated Neutrophilic Metamyelocyte	
Neutrophilic Band	Neutrophilic Band
Segmented Neutrophil	Segmented Neutrophil

Eosinophilic Myelocyte	Eosinophilic Myelocyte
Eosinophilic Metamyelocyte	Eosinophilic Metamyelocyte
Eosinophilic Band	Eosinophilic Band
Segmented Eosinophil	Segmented Eosinophil
Basophilic Metamyelocyte	Immature Basophil
Basophilic Band	
Basophilic Myelocyte	
Segmented Basophil	Segmented Basophil
Promonocyte	Immature Monocyte
Immature Monocyte	
Monocytic Blast	Monocytic Blast
Monocyte	Monocyte
Prolymphocyte	Immature Lymphocyte
Lymphoid Precursor Cell	
Lymphocytic Blast	Lymphocytic Blast
Lymphocyte	Lymphocyte
Proerythroblast	Proerythroblast Or Basophilic Erythroblast
Basophilic Erythroblast	
Polychromatic Erythroblast	Polychromatic Erythroblast
Orthochromatic Erythroblast	Orthochromatic Erythroblast
Megakaryocyte	Megakaryocyte
Thrombocyte	Thrombocyte
Thrombocyte Aggregate	
Giant Platelet	Giant Platelet
Neutrophil Extracellular Trap	Neutrophil Extracellular Trap
Pseudo Gaucher Cell	Pseudo Gaucher Cell

Mitosis	Mitosis
Spicule	Spicule
Erythrocyte	Other Cell
Plasma Cell	
Macrophage	
Lymphoidocyte	
Phagocytosis	
Micromegakaryocyte	
Promegakaryocyte	
Smudge Cell	
Artifact	Artifact
Damaged Cell	Not Identifiable
Technically Unfit	
Unknown Blast	

Supplemental Table 1: Mapping of the original cell class labels as created using the annotation application to the resulting 33 cell classes used for cell classification.

	COMPONENT	DISPLAY_NAME
LOINC		
14804-9	Lactate dehydrogenase	LDH Lactate to pyruvate reaction
1743-4	Alanine aminotransferase	ALT With P-5'-P [Catalytic activity/Vol]
20570-8	Hematocrit	Hematocrit (Bld) [Volume fraction]

2160-0	Creatinine	Creatinine [Mass/Vol]
28539-5	Erythrocyte mean corpuscular hemoglobin	MCH (RBC) [Entitic mass]
28540-3	Erythrocyte mean corpuscular hemoglobin concentration	MCHC (RBC) [Mass/Vol]
30239-8	Aspartate aminotransferase	AST With P-5'-P [Catalytic activity/Vol]
30385-9	Erythrocyte distribution width	Erythrocyte distribution width (RBC) [Ratio]
30428-7	Erythrocyte mean corpuscular volume	MCV (RBC) [Entitic vol]
3084-1	Urate	Urate [Mass/Vol]
6690-2	Leukocytes	WBC Auto (Bld) [# /Vol]
714-6	Eosinophils/100 leukocytes	Eosinophils/100 WBC Manual cnt (Bld)
718-7	Hemoglobin	Hemoglobin (Bld) [Mass/Vol]
737-7	Lymphocytes/100 leukocytes	Lymphocytes/100 WBC Manual cnt (Bld)
744-3	Monocytes/100 leukocytes	Monocytes/100 WBC Manual cnt (Bld)
769-0	Neutrophils.segmented/100 leukocytes	Segmented neutrophils/100 WBC Manual cnt (Bld)
777-3	Platelets	Platelets Auto (Bld) [# /Vol]
789-8	Erythrocytes	RBC Auto (Bld) [# /Vol]

Supplemental Table 2: List of laboratory values in the dataset as LOINC codes with their respective descriptions.

patient id	age	gender	leukemia_type	leukemia_sub_type	split	exclusion_reason_cell_classification	exclusion_reason_cell_detection	exclusion_reason_diagnostic_models
E2EF524FBF3D9FE611D5A8E90FEFDC9C	[4, 6[f	ALL	pro-B-ALL	train			
02E74F10E0327AD868D138F2B4FDD6F0	[16, 19[m	CML	Chronic Phase	train			No lab values available.
B53B3A3D6AB90CE0268229151C9BDE11	[8, 11[m	ALL	c-ALL	train	No cell classes annotated for this patient.		
C82561EC215A6E31807CEE DF3B3BD25E	[11, 14[f	CML	Chronic Phase	train			
F4B9EC30AD9F68F89B29639786CB62EF	[8, 11[f	ALL	pre-B-ALL	train			
A3F390D88E4C41F2747BFA2F1B5F87DB	[0, 3[f	ALL	intermediate cortical T-ALL	train			
68D30A9594728BC39AA24BE94B319D21	[4, 6[m	ALL	c-ALL	test			
3416A75F4CEA9109507CACD8E2F2AEFC	[16, 19[m	CML	Chronic Phase	validation			
4C56FF4CE4AAF9573AA5DF913DF997A	[11, 14[m	AML	AML M2	test	No cell classes annotated for this patient.		
A1D0C6E83F027327D8461063F4AC58A6	[8, 11[m	CML	Chronic Phase	validation			
34173CB38F07F89DDBEBC2AC9128303F	[11, 14[m	CML	Chronic Phase	test			
32BB90E8976AAB5298D5DA10FE66F21D	[4, 6[f	ALL	c-ALL	train			
3295C76ACBF4CAAED33C36B1B5FC2CB1	[4, 6[m	ALL	c-ALL	validation	No cell classes annotated for this patient.		
182BE0C5CDCD5072BB1864CDEE4D3D6E	[11, 14[f	CML	Chronic Phase	test			
DA4FB5C6E93E74D3DF8527599FA62642	[4, 6[m	ALL	c-ALL, co-expression	train			
B6D767D2F8ED5D21A44B0E5886680CB9	[6, 8[f	CML	Chronic Phase	train			
02522A2B2726FB0A03BB19F2D8D9524D	[0, 3[m	AML	AML M5	test			
A97DA629B098B75C294DFFDC3E463904	[3, 4[f	ALL	c-ALL, co-expression	train	No cell classes annotated for this patient.		
EC5DECCA5ED3D6B8079E2E7E7BACC9F2	[6, 8[m	AML	AML M2	validation			
19CA14E7EA6328A42E0EB13D585E4C22	[6, 8[m	CML	Chronic Phase	train			
7CBBC409EC990F19C78C75BD1E06F215	[6, 8[f	ALL	pre-B-ALL	train			
E4DA3B7FBBCE2345D7772B0674A318D5	[16, 19[m	CML	Chronic Phase	train			
F0935E4CD5920AA6C7C996A5EE53A70F	[4, 6[m	ALL	intermediate cortical T-ALL	train	No cell classes annotated for this patient.		Patient has already been under treatment at the time of the smear.
38B3EFF8BAF56627478EC76A704E9B52	[0, 3[m	ALL	pre-B-ALL	train			
AAB3238922BCC25A6F606EB525FFDC56	[16, 19[m	CML	Chronic Phase	validation			
A684ECEEE76FC522773286A895BC8436	[6, 8[m	ALL	intermediate cortical T-ALL	train	No cell classes annotated for this patient.		
EB160DE1DE89D9058FCB0B968DBBBD68	[14, 16[m	ALL	c-ALL	train			

1F0E3DAD99908345F7439F8 FFABDFFC4	[6, 8[f	CML	Chronic Phase	train		
ED3D2C21991E3BEF5E0697 13AF9FA6CA	[14, 16[f	ALL	c-ALL	train		
03AFDBD66E7929B125F859 7834FA83A4	[0, 3[m	ALL	pro-B-ALL	validation	No cell classes annotated for this patient.	
C8FFE9A587B126F152ED3D 89A146B445	[8, 11[m	AML	AML M4	test		
A87FF679A2F3E71D9181A67 B7542122C	[14, 16[m	CML	Chronic Phase	test		
6364D3F0F495B6AB9DCF8D 3B5C6E0B01	[8, 11[f	CML	Chronic Phase	train		
42A0E188F5033BC65BF8D7 8622277C4E	[0, 3[m	AML	AML M7	test	No cell classes annotated for this patient.	
C51CE410C124A10E0DB5E4 B97FC2AF39	[16, 19[m	CML	Chronic Phase	train		
C9F0F895FB98AB9159F51F D0297E236D	[14, 16[m	CML	Chronic Phase	train		
D2DDEA18F00665CE8623E3 6BD4E3C7C5	[3, 4[m	ALL	pre-B-ALL	train		
54229ABFCFA5649E7003B83 DD4755294	[11, 14[m	ALL	c-ALL	train		
C20AD4D76FE97759AA27A0 C99BFF6710	[16, 19[m	CML	Chronic Phase	train		
9BF31C7FF062936A96D3C8 BD1F8F2FF3	[14, 16[f	CML	Chronic Phase	test		No lab values available.
1C383CD30B7C298AB50293 ADFECB7B18	[16, 19[m	CML	Chronic Phase	train		
C81E728D9D4C2F636F067F 89CC14862C	[16, 19[m	CML	Chronic Phase	validation		
98DCE83DA57B0395E16346 7C9DAE521B	[4, 6[f	ALL	c-ALL	validation		
76DC611D6EBA AFC66CC08 79C71B5DB5C	[8, 11[f	AML	AML M4	train		
3C59DC048E8850243BE807 9A5C74D079	[14, 16[m	CML	Chronic Phase	test		
37693CFC748049E45D87B8 C7D8B9AACD	[8, 11[m	CML	Chronic Phase	train		
ECCBC87E4B5CE2FE28308 FD9F2A7BAF3	[8, 11[f	CML	Chronic Phase	train		
73278A4A86960EEB576A8F D4C9EC6997	[11, 14[f	ALL	c-ALL, co-expression	validation		
D82C8D1619AD8176D66545 3CFB2E55F0	[6, 8[f	ALL	pre-B-ALL	validation	No cell classes annotated for this patient.	
698D51A19D8A121CE58149 9D7B701668	[0, 3[m	ALL	pre-B-ALL	train		
5F93F983524DEF3DCA4644 69D2CF9F3E	[3, 4[f	ALL	c-ALL, co-expression	test		
7F1DE29E6DA19D22B51C68 001E7E0E54	[16, 19[m	AML	AML M4	validation		
1679091C5A880FAF6FB5E60 87EB1B2DC	[14, 16[m	CML	Chronic Phase	train		
AC627AB1CCBDB62EC96E7 02F07F6425B	[4, 6[f	ALL	c-ALL	train		
A5771BCE93E200C36F7CD9 DFD0E5DEAA	[8, 11[f	CML	Chronic Phase	train		No lab values available.
6F4922F45568161A8CDF4A D2299F6D23	[4, 6[f	CML	Blast Phase	train		
92CC227532D17E56E07902 B254DFAD10	[16, 19[m	ALL	c-ALL	train		
28DD2C7955CE926456240B 2FF0100BDE	[4, 6[f	ALL	c-ALL	validation	No cell classes annotated for this patient.	
66F041E16A60928B05A7E22 8A89C3799	[0, 3[f	ALL	c-ALL	validation	No cell classes annotated for this patient.	

65B9EEA6E1CC6BB9F0CD2 A47751A186F	[16, 19[f	ALL	c-ALL	train	No cell classes annotated for this patient.		
44F683A84163B3523AFE57C 2E008BC8C	[6, 8[m	ALL	intermediate cortical T-ALL	test			
33E75FF09DD601BBE69F35 1039152189	[8, 11[f	CML	Chronic Phase	train			
0F28B5D49B3020AFEEDC95 B4009ADF4C	[16, 19[m	AML	AML M3	train	No cell classes annotated for this patient.		
A5BFC9E07964F8DDDEB95 FC584CD965D	[8, 11[m	CML	Chronic Phase	train			
F033AB37C30201F73F14244 9D037028D	[4, 6[m	ALL	c-ALL	train			
07E1CD7DCA89A167804247 7183B7AC3F	[4, 6[f	ALL	intermediate cortical T-ALL	test	No cell classes annotated for this patient.		
069059B7EF840F0C74A814E C9237B6EC	[0, 3[m	AML	AML M5	validation			
98F13708210194C475687BE 6106A3B84	[11, 14[m	CML	Chronic Phase	train			
E369853DF766FA44E1ED0F F613F563BD	[16, 19[f	CML	Chronic Phase	train			
202CB962AC59075B964B071 52D234B70	[8, 11[f	AML	AML M2	train			
17E62166FC8586DFA4D1BC 0E1742C08B	[14, 16[m	CML	Chronic Phase	train			
C4CA4238A0B923820DCC50 9A6F75849B	[11, 14[m	CML	Chronic Phase	train			
E2C420D928D4BF8CE0FF2E C19B371514	[14, 16[m	ALL	pro-T-ALL	test			
8E296A067A37563370DED05 F5A3BF3EC	[16, 19[f	CML	Chronic Phase	test			
D1FE173D08E959397ADF34 B1D77E88D7	[8, 11[f	ALL	pre-B-ALL	validation			
642E92EFB79421734881B53 E1E1B18B6	[4, 6[m	CML	Chronic Phase	train			
9B8619251A19057CFF70779 273E95AA6	[14, 16[m	AML	AML M5	train			
EA5D2F1C4608232E07D3AA 3D998E5135	[0, 3[m	ALL	c-ALL	validation	No cell classes annotated for this patient.		
70EFD2EC9B086079795C4 42636B55FB	[8, 11[f	CML	Chronic Phase	train			
8EB6D8747175919F2747267 3A32B3ECA	[8, 11[m	CML	Blast Phase	test	No cell classes annotated for this patient.		
E00DA03B685A0DD18FB6A0 8AF0923DE0	[11, 14[m	AML	AML M1	train	No cell classes annotated for this patient.		
D3D9446802A44259755D38E 6D163E820	[14, 16[m	CML	Chronic Phase	validation			
14BFA6BB14875E45BBA028 A21ED38046	[0, 3[f	ALL	c-ALL	train			
D9D4F495E875A2E075A1A4 A6E1B9770F	[16, 19[m	CML	Chronic Phase	train			
7647966B7343C2904867325 2E490F736	[11, 14[f	ALL	pre-B-ALL	train			
65DED5353C5EE48D0B7D48 C591B8F430	[16, 19[m	AML	AML M2	train			
F899139DF5E105939643141 5E770C6DD	[3, 4[m	ALL	pre-B-ALL	test			
93DB85ED909C13838FF95C CFA94CEBD9	[0, 3[m	ALL	c-ALL	test			
72B32A1F754BA1C09B3695 E0CB6CDE7F	[4, 6[f	ALL	c-ALL	train	No cell classes annotated for this patient.		
AD61AB143223EFBC24C7D2 583BE69251	[4, 6[m	ALL	c-ALL	test			
A0A080F42E6F13B3A2DF13 3F073095DD	[8, 11[m	AML	AML M4	train	No cell classes annotated for this patient.		

1385974ED5904A438616FF7 BDB3F7439	[14, 16[f	AML	AML M1	test	No cell classes annotated for this patient.		
2838023A778DFAECDC2127 08F721B788	[3, 4[f	ALL	c-ALL, biphenotypic	test	No cell classes annotated for this patient.		
5FD0B37CD7DBBB00F97BA 6CE92BF5ADD	[16, 19[m	ALL	pre-B-ALL	test			
2B44928AE11FB9384C4CF3 8708677C48	[14, 16[f	ALL	pre-B-ALL, co-expression	test			
D1F491A404D6854880943E5 C3CD9CA25	[11, 14[f	AML	AML M2	train			
4E732CED3463D06DE0CA9 A15B6153677	[14, 16[m	CML	Chronic Phase	train			
C45147DEE729311EF5B5C3 003946C48F	[6, 8[m	ALL	c-ALL, co-expression	train			
D645920E395FEDAD7BBBE D0ECA3FE2E0	[11, 14[m	CML	Chronic Phase	train			
A3C65C2974270FD093EE8A 9BF8AE7D0B	[0, 3[m	ALL	c-ALL	train			
C16A5320FA475530D9583C3 4FD356EF5	[4, 6[m	CML	Chronic Phase	train			
2A38A4A9316C49E5A833517 C45D31070	[0, 3[f	ALL	c-ALL	train			
093F65E080A295F8076B1C5 722A46AA2	[6, 8[m	ALL	pre-B-ALL	validation	No cell classes annotated for this patient.		
7F6FFAA6BB0B408017B6225 4211691B5	[0, 3[f	ALL	c-ALL, co-expression	train			
F7177163C833DFF4B38FC8 D2872F1EC6	[8, 11[m	CML	Chronic Phase	test			
8F14E45FCEEA167A5A36DE DD4BEA2543	[14, 16[m	CML	Blast Phase	validation			
D67D8AB4F4C10BF22AA353 E27879133C	[8, 11[m	CML	Chronic Phase	train			No lab values available.
26657D5FF9020D2ABEFE55 8796B99584	[3, 4[m	ALL	c-ALL	test			
8613985EC49EB8F757AE643 9E879BB2A	[11, 14[m	ALL	intermediate cortical T-ALL	train			
2723D092B63885E0D7C260 CC007E8B9D	[6, 8[f	ALL	pro-B-ALL, co-expression	test			
6C8349CC7260AE62E3B139 6831A8398F	[14, 16[f	CML	Chronic Phase	train			
3988C7F88EBCB58C6CE932 B957B6F332	[11, 14[m	AML	AML M5	train			No lab values available. No clinical DCC available.
4443AEE183B279F76A95C13 C7F5BCA0D	[16, 19[m	CML	Blast Phase	test			
6974CE5AC660610B44D9B9 FED0FF9548	[14, 16[m	ALL	c-ALL	validation			
7F39F8317FBDB1988EF4C6 28EBA02591	[0, 3[m	ALL	c-ALL	train			
C7E1249FFC03EB9DED908 C236BD1996D	[4, 6[m	ALL	pre-B-ALL	train			
45C48CCE2E2D7FBDEA1AF C51C7C6AD26	[16, 19[f	CML	Chronic Phase	train			
67C6A1E7CE56D3D6FA748A B6D9AF3FD7	[14, 16[m	CML	Chronic Phase	validation			
EC8956637A99787BD197EA CD77ACCE5E	[0, 3[f	ALL	pro-B-ALL	test			
D09BF41544A3365A46C9077 EBB5E35C3	[11, 14[m	ALL	c-ALL	test			
6512BD43D9CAA6E02C990B 0A82652DCA	[4, 6[m	CML	Blast Phase	train			
43EC517D68B6EDD3015B3E DC9A11367B	[3, 4[m	ALL	c-ALL	test			

FC490CA45C00B1249BBE35 54A4FDF6FB	[4, 6[f	ALL	intermediate cortical T-ALL	validation	No cell classes annotated for this patient.		
072B030BA126B2F4B2374F3 42BE9ED44	[8, 11[m	ALL	pre-B-ALL	test	No cell classes annotated for this patient.		
C0C7C76D30BD3DCAEFC96 F40275BDC0A	[14, 16[f	CML	Chronic Phase	train			
5EF059938BA799AAA845E1 C2E8A762BD	[14, 16[m	ALL	c-ALL	train			
A6BBC91AE73DD21C0533F7 35470A9CD0	[16, 19[f	CML	Chronic Phase	train			
C74D97B01EAE257E44AA9D 5BADE97BAF	[16, 19[m	CML	Chronic Phase	validation			
9F61408E3AFB633E50CDF1 B20DE6F466	[4, 6[m	ALL	c-ALL	train	No cell classes annotated for this patient.		
FBD7939D674997CDB4692D 34DE8633C4	[3, 4[m	ALL	intermediate cortical T-ALL	train			
9FC3D7152BA9336A670E36 D0ED79BC43	[16, 19[f	AML	AML M2	train			
9A1158154DFA42CADDDBD06 94A4E9BDC8	[3, 4[f	ALL	c-ALL	train	No cell classes annotated for this patient.		
3DEF184AD8F4755FF269862 EA77393DD	[14, 16[f	AML	AML M3	test			
C7FF6173CE74C106F0871C EA7F91F152	[6, 8[ALL	Burkitt leukemia	validation	No cell classes annotated for this patient.		No lab values available.
3B80517688B93186611E64F E9268FCA7	[8, 11[ALL	Burkitt leukemia	train	No cell classes annotated for this patient.		
700049AE9F8CB7635BF38E A93D450C00	[14, 16[ALL	Burkitt leukemia	test	No cell classes annotated for this patient.		
0A09C8844BA8F0936C20BD 791130D6B6	[16, 19[m	AML	AML M1	train			No lab values available. No clinical DCC available.
2B24D495052A8CE66358EB 576B8912C8	[4, 6[f	AML		train			No lab values available. No clinical DCC available.
8D5E957F297893487BD98FA 830FA6413	[14, 16[f	AML	AML M3	test			No lab values available. No clinical DCC available.
47D1E990583C9C67424D369 F3414728E	[11, 14[m	AML	AML M3	train			No lab values available. No clinical DCC available.
F2217062E9A397A1DCA429 E7D70BC6CA	[3, 4[m	AML	AML M5	train			No lab values available. No clinical DCC available.
7EF605FC8DBA5425D6965F BD4C8FBE1F	[4, 6[m	AML		test			No lab values available. No clinical DCC available.
A8F15EDA80C50ADB0E7194 3ADC8015CF	[0, 3[m	AML		validation			No lab values available. No clinical DCC available.
37A749D808E46495A8DA1E 5352D03CAE	[0, 3[f	AML	AML M7	train	No cell classes annotated for this patient.		No lab values available. No clinical DCC available.
B3E3E393C77E35A4A3F3CB D1E429B5DC	[16, 19[f	AML	AML M2	train	No cell classes annotated for this patient.		No lab values available. No clinical DCC available.

2A79EA27C279E471F4D180 B08D62B00A	[11, 14[f	AML	AML M1	validation	No cell classes annotated for this patient.	No lab values available. No clinical DCC available.
1C9AC0159C94D8D0CBEDC 973445AF2DA	[0, 3[f	AML	AML M4	validation	No cell classes annotated for this patient.	No lab values available. No clinical DCC available.
6C4B761A28B734FE93831E3 FB400CE87	[8, 11[f	AML	AML M1	train	No cell classes annotated for this patient.	No lab values available. No clinical DCC available.
06409663226AF2F3114485A A4E0A23B4	[0, 3[f	AML	AML M5	test	No cell classes annotated for this patient.	No lab values available. No clinical DCC available.
140F6969D5213FD0ECE031 48E62E461E	[6, 8[m	AML	AML M1	test	No cell classes annotated for this patient.	No lab values available. No clinical DCC available.
B73CE398C39F506AF761D2 277D853A92	[0, 3[m	AML	AML M7	validation	No cell classes annotated for this patient.	No lab values available. No clinical DCC available.
BD4C9AB730F5513206B999 EC0D90D1FB	[8, 11[f	AML	AML M2	validation	No cell classes annotated for this patient.	No lab values available. No clinical DCC available.
82AA4B0AF34C2313A562076 992E50AA3	[14, 16[m	AML	AML M1	train	No cell classes annotated for this patient.	No lab values available. No clinical DCC available.
0777D5C17D4066B82AB86D FF8A46AF6F	[11, 14[f	AML	AML M2	test	No cell classes annotated for this patient.	No lab values available. No clinical DCC available.
9766527F2B5D3E95D4A733F CFB77BD7E	[3, 4[f	AML	AML M3	validation	No cell classes annotated for this patient.	No lab values available. No clinical DCC available.
7E7757B1E12ABCB736AB9A 754FFB617A	[0, 3[f	AML	AML M7	train	No cell classes annotated for this patient.	No lab values available. No clinical DCC available.
5878A7AB84FB43402106C57 5658472FA	[0, 3[f	AML	AML M7	validation	No cell classes annotated for this patient.	No lab values available. No clinical DCC available.
006F52E9102A8D3BE2FE56 14F42BA989	[11, 14[f	AML	AML M2	train	No cell classes annotated for this patient.	No lab values available. No clinical DCC available.
3636638817772E42B59D74C FF571FBB3	[3, 4[f	AML	AML M3	train	No cell classes annotated for this patient.	No lab values available. No clinical DCC available.
149E9677A5989FD342AE442 13DF68868	[0, 3[f	AML	AML M7	train	No cell classes annotated for this patient.	No lab values available. No clinical DCC available.
A4A042CF4FD6BFB47701CB C8A1653ADA	[0, 3[f	AML	AML M4	test	No cell classes annotated for this patient.	No lab values available. No clinical DCC available.

BF8229696F7A3BB4700CFD DEF19FA23F	[0, 3[f	AML	AML M4	train	No cell classes annotated for this patient.	No lab values available. No clinical DCC available.
82161242827B703E6ACF9C7 26942A1E4	[0, 3[f	AML	AML M7	train	No cell classes annotated for this patient.	No lab values available. No clinical DCC available.
8F85517967795EEEF66C225 F7883BDCB	[16, 19[f	AML	AML M0	test	No cell classes annotated for this patient.	No lab values available.
FC221309746013AC554571F BD180E1C8	[8, 11[m	AML	AML M0	train	No cell classes annotated for this patient.	No lab values available.
31FEFC0E570CB3860F2A6D 4B38C6490D	[16, 19[m	AML	AML M1	validation	No cell classes annotated for this patient.	No lab values available. No clinical DCC available.
9DCB88E0137649590B75537 2B040AFAD	[14, 16[m	AML	AML M1	train	No cell classes annotated for this patient.	No lab values available. No clinical DCC available.
0AA1883C6411F7873CB83D ACB17B0AFC	[14, 16[f	AML	AML M1	test	No cell classes annotated for this patient.	No lab values available.
A597E50502F5FF68E3E25B9 114205D4A	[14, 16[AML	AML M1	train	No cell classes annotated for this patient.	No lab values available. No clinical DCC available.
0336DCBAB05B9D5AD24F43 33C7658A0E	[4, 6[AML	AML M1	train	No cell classes annotated for this patient.	No lab values available.
BD686FD640BE98EFAAE009 1FA301E613	[14, 16[f	AML	AML M1	train	No cell classes annotated for this patient.	No lab values available.
58A2FC6ED39FD083F55D41 82BF88826D	[14, 16[f	AML	AML M1	validation	No cell classes annotated for this patient.	No lab values available.
084B6FBB10729ED4DA8C3D 3F5A3AE7C9	[11, 14[m	AML	AML M1	test	No cell classes annotated for this patient.	No lab values available.
84D9EE44E457DDEF7F2C4F 25DC8FA865	[3, 4[f	AML	AML M1	train	No cell classes annotated for this patient.	No lab values available.
3644A684F98EA8FE223C713 B77189A77	[14, 16[f	AML	AML M1	train	No cell classes annotated for this patient.	No lab values available.
E2C0BE24560D78C5E599C2 A9C9D0BBD2	[8, 11[m	AML	AML M2	validation	No cell classes annotated for this patient.	No lab values available.
274AD4786C3ABCA69FA097 B85867D9A4	[6, 8[m	AML	AML M2	train	No cell classes annotated for this patient.	No lab values available.
EAE27D77CA20DB309E056E 3D2DCC7D69	[8, 11[f	AML	AML M2	train	No cell classes annotated for this patient.	No lab values available. No clinical DCC available.
69ADC1E107F7F7D035D7BA F04342E1CA	[6, 8[f	AML	AML M2	validation	No cell classes annotated for this patient.	No lab values available.
091D584FCED301B442654D D8C23B3FC9	[6, 8[m	AML	AML M2	test	No cell classes annotated for this patient.	No lab values available.
B1D10E7BAFA4421218A51B 1E1F1B0BA2	[8, 11[f	AML	AML M2	train	No cell classes annotated for this patient.	No lab values available.
979D472A84804B9F647BC18 5A877A8B5	[11, 14[f	AML	AML M2	test	No cell classes annotated for this patient.	No lab values available.
CA46C1B9512A7A8315FA3C 5A946E8265	[3, 4[f	AML	AML M2	train	No cell classes annotated for this patient.	No lab values available.
3B8A614226A953A8CD9526 FCA6FE9BA5	[16, 19[m	AML	AML M2	train	No cell classes annotated for this patient.	No lab values available.
63DC7ED1010D3C3B8269FA F0BA7491D4	[16, 19[f	AML	AML M2	validation	No cell classes annotated for this patient.	No lab values available.
E96ED478DAB8595A7DBDA 4CBCBEE168F	[4, 6[f	AML	AML M2	train	No cell classes annotated for this patient.	No lab values available.
6F3EF77AC0E3619E98159E 9B6FEBF557	[11, 14[m	AML	AML M2	train	No cell classes annotated for this patient.	No lab values available.

D1C38A09ACC34845C6BE3 A127A5AACAF	[8, 11[f	AML	AML M3	train	No cell classes annotated for this patient.		No lab values available.
EC8CE6ABB3E952A85B8551 BA726A1227	[14, 16[m	AML	AML M3	train	No cell classes annotated for this patient.		No lab values available.
060AD92489947D410D89747 4079C1477	[14, 16[m	AML	AML M3	validation	No cell classes annotated for this patient.		No lab values available.
C0E190D8267E36708F955D7 AB048990D	[11, 14[f	AML	AML M3	test	No cell classes annotated for this patient.		No lab values available.
9B04D152845EC0A37839400 3C96DA594	[14, 16[f	AML	AML M4	train	No cell classes annotated for this patient.		No lab values available.
74DB120F0A8E5646EF5A30 154E9F6DEB	[3, 4[m	AML	AML M4	test	No cell classes annotated for this patient.		No lab values available.
E56954B4F6347E897F95449 5EAB16A88	[0, 3[f	AML	AML M4Eo	train	No cell classes annotated for this patient.		No lab values available.
EDA80A3D5B344BC40F3BC 04F65B7A357	[0, 3[m	AML	AML M4Eo	train	No cell classes annotated for this patient.		No lab values available.
8F121CE07D74717E0B1F21 D122E04521	[11, 14[m	AML	AML M4Eo	validation	No cell classes annotated for this patient.		No lab values available.
06138BC5AF6023646EDE0E 1F7C1EAC75	[11, 14[f	AML	AML M4Eo	test	No cell classes annotated for this patient.		No lab values available.
39059724F73A9969845DFE4 146C5660E	[6, 8[m	AML	AML M4Eo	train	No cell classes annotated for this patient.		No lab values available.
7F100B7B36092FB9B06DFB 4FAC360931	[16, 19[AML	AML M4Eo	train	No cell classes annotated for this patient.		No lab values available.
7A614FD06C325499F1680B9 896BEEDEB	[16, 19[m	AML	AML M4Eo	train	No cell classes annotated for this patient.		No lab values available.
335F5352088D7D9BF74191E 006D8E24C	[8, 11[f	AML	AML M5	train	No cell classes annotated for this patient.		No lab values available.
E4A6222CDB5B34375400904 F03D8E6A5	[0, 3[f	AML	AML M5	train	No cell classes annotated for this patient.		No lab values available.
CB70AB375662576BD1AC5A AF16B3FCA4	[16, 19[f	AML	AML M5	validation	No cell classes annotated for this patient.		No lab values available.
38DB3AED920CF82AB059BF CCBD02BE6A	[3, 4[f	AML	AML M5	test	No cell classes annotated for this patient.		No lab values available.
621BF66DDB7C962AA0D22A C97D69B793	[0, 3[m	AML	AML M5	train	No cell classes annotated for this patient.		No lab values available.
C24CD76E1CE41366A4BBE8 A49B02A028	[0, 3[m	AML	AML M6	test	No cell classes annotated for this patient.		No lab values available.
03C6B06952C750899BB03D 998E631860	[0, 3[m	AML	AML M6	train	No cell classes annotated for this patient.		No lab values available.
C52F1BD66CC19D05628BD8 BF27AF3AD6	[0, 3[m	AML	AML M7	test	No cell classes annotated for this patient.		No lab values available.
B1A59B315FC9A3002CE38B BE070EC3F5	[4, 6[f	AML	AML M7	train	No cell classes annotated for this patient.		No lab values available.
D96409BF894217686BA124D 7356686C9	[0, 3[m	AML	AML M7	validation	No cell classes annotated for this patient.		No lab values available.
36660E59856B4DE58A219B CF4E27EBA3	[0, 3[m	AML	AML M7	train	No cell classes annotated for this patient.		No lab values available.
2EAB84C785399B2DCDD75F D40917C17C	[4, 6[f	ALL	pre-B-ALL, co-expression	train	No cell classes annotated for this patient.	No cell boxes annotated for this patient.	No lab values available. No clinical DCC available.
398499203B70C029E7F1BEF F75C0DEA1	[0, 3[m	ALL	pre-B-ALL, co-expression	train	No cell classes annotated for this patient.	No cell boxes annotated for this patient.	No lab values available. No clinical DCC available.
BA6484A665B9A691A37F578 72C643E04	[14, 16[m	ALL	pro-B-ALL, co-expression	train	No cell classes annotated for this patient.	No cell boxes annotated for this patient.	No lab values available. No clinical DCC available.
F768F6C7948E6A750060AF1 5FB73BF6C	[4, 6[m	ALL	c-ALL, co-expression	test	No cell classes annotated for this patient.	No cell boxes annotated for this patient.	No lab values available. No clinical DCC available.

5C820C4E9439DC590E3192 DBB774255E	[0, 3[f	ALL	pre-B-ALL, co-expression	train	No cell classes annotated for this patient.	No cell boxes annotated for this patient.	No lab values available. No clinical DCC available.
F0549529AF3E0E57F00F30C F1E1FC994	[8, 11[f	ALL	c-ALL, co-expression	test	No cell classes annotated for this patient.	No cell boxes annotated for this patient.	No lab values available. No clinical DCC available.
F7405A633A5F7482725CC94 B3563A5B6	[4, 6[f	ALL	c-ALL, co-expression	validation	No cell classes annotated for this patient.	No cell boxes annotated for this patient.	No lab values available. No clinical DCC available.
399C0FDBA7E789C6736AC6 60D23B4BB6	[4, 6[m	ALL	c-ALL, co-expression	validation	No cell classes annotated for this patient.	No cell boxes annotated for this patient.	No lab values available. No clinical DCC available.
3421557EEC62C83EEA2C83 C08A79CDB9	[0, 3[f	ALL	c-ALL, co-expression	train	No cell classes annotated for this patient.	No cell boxes annotated for this patient.	No lab values available. No clinical DCC available.
BCDCEF5EF4CF9871F0CB6 BFF04753754	[0, 3[f	ALL	pre-B-ALL, co-expression	test	No cell classes annotated for this patient.	No cell boxes annotated for this patient.	No lab values available. No clinical DCC available.
1A00B3B296CD48BA5D1BD7 6B18C48346	[0, 3[m	ALL	pro-B-ALL, co-expression	validation	No cell classes annotated for this patient.	No cell boxes annotated for this patient.	No lab values available. No clinical DCC available.
12ED127BACFF11D62A255B E81C5E2310	[4, 6[m	ALL	c-ALL, co-expression	train	No cell classes annotated for this patient.	No cell boxes annotated for this patient.	No lab values available. No clinical DCC available.
47397D3C4DB6F903852E876 60CB96E3D	[4, 6[m	ALL	c-ALL, co-expression	train	No cell classes annotated for this patient.	No cell boxes annotated for this patient.	No lab values available. No clinical DCC available.
BB8CF22800F0D97AB7EC98 F1213B4B4E	[6, 8[f	ALL	pre-B-ALL, co-expression	validation	No cell classes annotated for this patient.	No cell boxes annotated for this patient.	No lab values available. No clinical DCC available.
4F584FE84E3D2EDE914508 A873D75855	[3, 4[f	ALL	c-ALL, biphenotypic	train	No cell classes annotated for this patient.	No cell boxes annotated for this patient.	No lab values available. No clinical DCC available.
357AAD4942E92FCC103D92 33B6739697	[0, 3[f	ALL	pro-B-ALL	train	No cell classes annotated for this patient.	No cell boxes annotated for this patient.	No lab values available. No clinical DCC available.
B4A67623E7A47A4406DECA C8E1A1DD6F	[6, 8[f	ALL	c-ALL, biphenotypic	validation	No cell classes annotated for this patient.	No cell boxes annotated for this patient.	No lab values available. No clinical DCC available.
002BD524C907A2A5121D3A DAED05D442	[11, 14[f	ALL	intermediate cortical T-ALL	train	No cell classes annotated for this patient.	No cell boxes annotated for this patient.	No lab values available. No clinical DCC available.
A61D1A964CA038E6FB5416 A8ECF0C76D	[8, 11[f	ALL	intermediate cortical T-ALL	train	No cell classes annotated for this patient.	No cell boxes annotated for this patient.	No lab values available. No clinical DCC available.
EAA51AE97DBF78D298CB4 BA55761AB8B	[11, 14[m	ALL	pro-T-ALL	train	No cell classes annotated for this patient.	No cell boxes annotated for this patient.	No lab values available. No clinical DCC available.

93ED4838BE11F21D2E5A8A03B36CD6BD	[8, 11[m	ALL	c-ALL, co-expression	train	No cell classes annotated for this patient.	No cell boxes annotated for this patient.	No lab values available. No clinical DCC available.
61BEED9E2C7DBF9CF3F2DBA9FFD26B2A	[6, 8[m	ALL	c-ALL, co-expression	train	No cell classes annotated for this patient.	No cell boxes annotated for this patient.	No lab values available. No clinical DCC available.
C24D731AC18944F0AFF1DBCCF40ED102	[4, 6[m	ALL	intermediate cortical T-ALL	train	No cell classes annotated for this patient.	No cell boxes annotated for this patient.	No lab values available. No clinical DCC available.
ACC68D832D90A3AAA9E2A38A529C62EB	[11, 14[f	ALL	c-ALL, co-expression	train	No cell classes annotated for this patient.	No cell boxes annotated for this patient.	No lab values available. No clinical DCC available.
9461E2E0784D432D5FD84528FDBC3BBE	[6, 8[m	ALL	intermediate cortical T-ALL	train	No cell classes annotated for this patient.	No cell boxes annotated for this patient.	No lab values available. No clinical DCC available.
D25E9132CF24B8A7A2164885101E62CB	[16, 19[f	ALL	pro-T-ALL	validation	No cell classes annotated for this patient.	No cell boxes annotated for this patient.	No lab values available. No clinical DCC available.
8963A6178314866F22F870E84026D429	[16, 19[m	ALL	intermediate cortical T-ALL	test	No cell classes annotated for this patient.	No cell boxes annotated for this patient.	No lab values available. No clinical DCC available.
12F54ACB6F92C80EAC9609D202A98325	[4, 6[f	ALL	intermediate cortical T-ALL	test	No cell classes annotated for this patient.	No cell boxes annotated for this patient.	No lab values available. No clinical DCC available.
75612D01831B0B8C48530A878109A865	[6, 8[m	ALL	intermediate cortical T-ALL	validation	No cell classes annotated for this patient.	No cell boxes annotated for this patient.	No lab values available. No clinical DCC available.
06FEE55734DEFE2EF2A60DEFFFD994FE	[14, 16[m	ALL	intermediate cortical T-ALL	validation	No cell classes annotated for this patient.	No cell boxes annotated for this patient.	No lab values available. No clinical DCC available.
C912541E67CD22445ED91775B8E89A7D	[14, 16[f	ALL	Burkitt leukemia	train	No cell classes annotated for this patient.	No cell boxes annotated for this patient.	No lab values available. No clinical DCC available.
87D5BE18C3F5EA9721B8B343120CD71C	[11, 14[m	ALL	Burkitt leukemia	train	No cell classes annotated for this patient.	No cell boxes annotated for this patient.	No lab values available. No clinical DCC available.
9A15F38C5291BA675D2E6DDF530BA6D9	[8, 11[m	ALL	Burkitt leukemia	validation	No cell classes annotated for this patient.	No cell boxes annotated for this patient.	No lab values available. No clinical DCC available.
623AE0B81861352D483A3CAE6CD34DDB	[8, 11[m	ALL	Burkitt leukemia	test	No cell classes annotated for this patient.	No cell boxes annotated for this patient.	No lab values available. No clinical DCC available.
FFD52F3C7E12435A724A8F30FDDADD9C	[0, 3[f	AML	AML M0	validation	No cell classes annotated for this patient.	No cell boxes annotated for this patient.	No lab values available. No clinical DCC available.

Supplemental Table 3: Clinical data and stratification of patients, as well as information about exclusion of specific patients from certain tasks.

Cell Class	F1	Recall	Precision
Myeloid Precursor Cell	0.409 (0.186-0.649)	0.409 (0.208-0.667)	0.409 (0.149-0.697)
Myelocytic Blast	0.490 (0.154-0.694)	0.489 (0.129-0.764)	0.492 (0.155-0.674)
Promyelocyte	0.799 (0.765-0.843)	0.850 (0.795-0.911)	0.754 (0.694-0.802)
Neutrophilic Myelocyte	0.543 (0.458-0.628)	0.543 (0.430-0.644)	0.543 (0.448-0.626)
Neutrophilic Metamyelocyte	0.588 (0.519-0.661)	0.589 (0.488-0.673)	0.586 (0.507-0.662)
Neutrophilic Band	0.724 (0.678-0.770)	0.745 (0.679-0.810)	0.704 (0.656-0.753)
Segmented Neutrophil	0.907 (0.885-0.927)	0.882 (0.850-0.916)	0.933 (0.897-0.959)
Eosinophilic Myelocyte	0.731 (0.566-0.839)	0.850 (0.629-0.977)	0.642 (0.481-0.763)
Eosinophilic Metamyelocyte	0.194 (0.000-0.485)	0.158 (0.000-0.473)	0.250 (0.000-0.600)
Eosinophilic Band	0.286 (0.080-0.539)	0.267 (0.063-0.636)	0.308 (0.091-0.566)
Segmented Eosinophil	0.720 (0.613-0.875)	0.726 (0.519-0.868)	0.714 (0.549-0.897)
Immature Basophil	0.250 (0.000-0.646)	0.176 (0.000-0.500)	0.429 (0.000-1.000)
Segmented Basophil	0.615 (0.420-0.799)	0.600 (0.370-0.861)	0.632 (0.348-0.811)
Immature Monocyte	0.261 (0.000-0.539)	0.176 (0.000-0.400)	0.500 (0.000-1.000)
Monocytic Blast	0.358 (0.138-0.630)	0.370 (0.132-0.639)	0.347 (0.118-0.654)
Monocyte	0.241 (0.089-0.471)	0.189 (0.060-0.403)	0.333 (0.130-0.660)
Immature Lymphocyte	0.000 (0.000-0.000)	0.000 (0.000-0.000)	0.000 (0.000-0.000)
Lymphocytic Blast	0.886 (0.853-0.922)	0.924 (0.887-0.962)	0.851 (0.803-0.894)
Lymphocyte	0.450 (0.272-0.604)	0.417 (0.248-0.591)	0.490 (0.266-0.688)
Proerythroblast or Basophilic Erythroblast	0.439 (0.218-0.683)	0.643 (0.300-0.928)	0.333 (0.143-0.610)

Polychromatic Erythroblast	0.648 (0.506-0.821)	0.719 (0.531-0.899)	0.590 (0.439-0.800)
Orthochromatic Erythroblast	0.764 (0.667-0.850)	0.714 (0.600-0.821)	0.821 (0.693-0.917)
Megakaryocyte	0.945 (0.888-0.986)	0.992 (0.952-1.000)	0.903 (0.806-0.980)
Thrombocyte	0.931 (0.874-0.970)	0.899 (0.830-0.954)	0.965 (0.881-0.994)
Giant Platelet	0.129 (0.000-0.387)	0.143 (0.000-0.441)	0.118 (0.000-0.480)
Neutrophil Extracellular Trap	0.876 (0.818-0.939)	0.878 (0.794-0.949)	0.874 (0.808-0.942)
Pseudo Gaucher Cell	0.667 (0.308-1.000)	0.800 (0.167-1.000)	0.571 (0.273-1.000)
Mitosis	0.692 (0.430-0.901)	0.692 (0.385-0.923)	0.692 (0.310-1.000)
Spicule	0.938 (0.880-0.970)	0.953 (0.843-1.000)	0.924 (0.833-0.978)
Other Cell	0.794 (0.630-0.891)	0.718 (0.559-0.836)	0.889 (0.657-0.987)
Smudge Cell	0.676 (0.576-0.756)	0.722 (0.638-0.802)	0.635 (0.522-0.734)
Artifact	0.557 (0.466-0.657)	0.582 (0.470-0.693)	0.534 (0.422-0.643)
Not Identifiable	0.531 (0.465-0.597)	0.474 (0.403-0.549)	0.602 (0.510-0.671)

Supplemental Table 4: Precision, recall, and F1-scores including 95% confidence intervals (BCa bootstrap) of the cell classifier per class.